Resonant Transition Based Quantum Computation

Chen-Fu Chiang [*], Chang-Yu Hsieh [†‡]

December 20, 2016

Abstract

In this article we assess a novel quantum computation paradigm based on the resonant transition (RT) phenomenon commonly associated with atomic and molecular systems. We thoroughly analyze the intimate connections between the RT-based quantum computation and the well-established adiabatic quantum computation (AQC). Both quantum computing frameworks encode solutions to computational problems in the spectral properties of a Hamiltonian and rely on the quantum dynamics to obtain the desired output state. We discuss how one can adapt any adiabatic quantum algorithm to a corresponding RT version and the two approaches are limited by different aspects of Hamiltonians' spectra. The RT approach provides a compelling alternative to the AQC under various circumstances. To better illustrate the usefulness of the novel framework, we analyze the time complexity of an algorithm for 3-SAT problems and discuss straightforward methods to fine tune its efficiency.

1 Introduction

In the past decades there has been a great progress in quantum computation. One of the aims of quantum computation is to attack computationally hard problems that prove difficult (if not impossible) for classical computers. Several quantum algorithms, such as Deutsch-Jozsa algorithm [1] and Shor's factoring algorithm[2], that provide exponential speed-up in comparison to the classical counterparts, have already been found and demonstrate the superiority of quantum computations.

Most early algorithm developments were based on the quantum circuit models in which qubits are operated by a sequence of discrete quantum gates in analogy to the classical circuit models. However, the complexity of quantum circuit models has deterred subsequent developments. A variety of alternative quantum computation models have been proposed to carry out quantum computations without explicitly relying on a circuit model. Among them, the adiabatic quantum computation (AQC) model [3, 4, 5, 6] is probably the most well-known and receives most attention. In this work, we shall compare a recently proposed quantum computation model to the AQC and discuss how this new model can be a practical alternative and complement to the AQC.

In a series of recent works, a new quantum computation model is introduced. In Ref. [7], a *polynomial* quantum algorithm for obtaining the energy spectrum of a physical system was proposed

[*]Department of Computer Science, State University of New York Polytechnic Institute, Utica, NY 13502, USA. Email:chiangc@sunyit.edu

[†]Department of Chemistry, Massachusetts Institute of Technology, Cambridge, MA 02139, USA. Email:changyuh@mit.edu

[‡]The order is based on the alphabetical order of the first letter of last name.

that can be used for phase estimation algorithm. Subsequently, Wang et al.,[8] generalized the model to solve 3-bit exact cover (EC3) problems and improved upon the earlier work on the phase estimation algorithm including the extraction of eigenstates of a Hamiltonian.

This new quantum computation framework is inspired by resonant transition (RT) phenomenon commonly observed in atomic and molecular systems. When a quantum system is only weakly perturbed, the system responds most actively when the perturbations resonate with some transition frequencies of the system's spectrum. Based on this principle, the computational problem is then encoded to the spectral properties of a Hamiltonian of the system and an external agent, a probe qubit, is brought into interaction with the system. By adjusting the property of the probe qubit, one can induce specific transitions inside the system and explore the eigen-energy of the system and eigenstates.

Despite relying on different physical processes, the RT model is actually intimately related to the well-established and highly successful AQC model. To clearly illustrate their connections, we (1) discuss how one can adapt any adiabatic algorithm to a corresponding RT algorithm and (2) inspect the underlying quantum dynamics of RT model and compare to that of the AQC model. As will become clear in the later discussions, the RT model suffers a potential performance hit when the spectrum of the Hamiltonian contains too many degenerate levels other than the manifold in which the solution (to a computational problem) is encoded. Since no adiabaticity is imposed onto the quantum dynamics, the RT model is significantly less susceptible to common obstacles such as the spectral gap issue[10] for the AQC model. Because of the high compatibility in terms of algorithm development and entirely different sources of obstacles in carrying out these quantum dynamics driven computations, we expect the RT model can provide a practical alternative and complement to the AQC. Towards the end, we show how RT algorithms perform in a non-trivial algorithmic context when we consider a 3-SAT problem. It will also be clear that the RT algorithm is clearly derived from an adiabatic version[5].

The structure of this work is described as the following. In section 2, we characterize the basics of the resonant-transition (RT) model based quantum computation. Explanations are then given on the structure of a RT-based EC3-solving algorithm and its physical implementations through Pauli matrices. In section 3, we review the essences of the AQC and the adiabatic path. Later we compare the quantum dynamics of the AQC with that of the RT-based quantum computation from the similarity perspective, the difference perspective and the performance perspective. Subsequently we demonstrate how to emulate the RT-based quantum computation via AQC. In section 4.1, we propose a new energy function to encode 3-SAT instances to be used in the EC3-solving algorithm to solve 3-SAT problems. The modified EC3-solving algorithm has a lower decay error probability and avoids the high degeneracy issue. We provide the performance analysis in section 4.2 and discussion in section 5.

2 Quantum Computation by The Resonant Transition Model

In this section, we explain the basic physics behind the RT model, illustrate the RT-based quantum computations through the original EC3-solving algorithm [8], and discuss its physical implementations and other characteristics.

2.1 Resonant Transition Physics

We present background material on the model system and the phenomenon of resonant transitions between two quantum states in order to make the present paper self-contained. To be elucidated in the subsequent section, the proposed quantum algorithms are realized physically with the resonant transitions of a quantum system coupled to an external agent.

Following [7, 8], we consider a quantum device composed of two sets of qubits, namely, the probe qubits and the register qubits. The register qubits could be constructed with an ensemble of two-level atoms in a cavity or trapped ions, while the probe qubits are additional two-level system supposed to possess highly adjustable physical properties, such as the resonant frequency and the coupling strength to the register qubits. For the rest of this paper, we should restrict the discussion to one probe qubit.

Similar to the Jaynes-Cummings model in quantum optics, this quantum device is described by the following Hamiltonian,

$$\begin{aligned} H &= H_p + H_s + H_{int} \\ &= \frac{1}{2}\omega_0 Z \otimes I_2^s + I_2 \otimes H_s + cX \otimes A, \end{aligned} \tag{1}$$

where H_s represents the many-body Hamiltonian for the quantum register, Z and X are standard Pauli matrices, and A denotes the probing operation on the quantum register due to interaction with the probe qubit. In this device, the probe qubit is governed by a particularly simple Hamiltonian, H_p, which sets the energy gap, ω_0, between the two states $|0\rangle$ and $|1\rangle$. The interaction with the quantum register should eventually result in a flip of the probe qubit's state from $|0\rangle$ to $|1\rangle$ or vice versa due to X appearing at the very last term in Eq. (1). We shall see shortly that the operator A generalizes X to induce transitions among quantum states of a multi-level quantum system.

Given the Hamiltonian in Eq. (1), the dynamics of the entire system (the register qubits plus the probe qubit) is governed by the unitary evolution $U(t) = \exp(-iHt)$. The time-evolved quantum state at time τ reads

$$\begin{aligned} \rho_\tau &= U(\tau)\rho_0 U^\dagger(\tau) \\ &= U(\tau)(|1\rangle\langle 1| \otimes |\Psi_s\rangle\langle\Psi_s|)U^\dagger(\tau), \end{aligned} \tag{2}$$

where $\rho_0 = |1\rangle\langle 1| \otimes |\Psi_s\rangle\langle\Psi_s|$ is the joint initial state. A transition in the probe qubit's state (say, from $|1\rangle$ to $|0\rangle$) is accompanied with a similar transition between states of the register qubits. The decay probability for the probe qubit can be quantitatively estimated from the perturbation theory,

$$P_{decay} = \langle 0| \operatorname{Tr}_s(\rho_\tau) |0\rangle , \tag{3}$$

where $\operatorname{Tr}_s(\cdot)$ denotes a partial trace over the register qubits. To implement the quantum algorithm, we operate the quantum device in the weak coupling limit, i.e. $c \ll 1$ in Eq. (1). In this scenario, the virtual transitions are strongly suppressed and the dominant pathways are the classical-like transitions in which energy is transferred back and forth from the probe qubit to the register qubits. One can approximately decompose Eq. (3) into an incoherent summation (i.e. no quantum interference) of distinct transitions between the i-th and j-th eigenstates of H_s. More precisely, the contribution to the decay probability of a particular transition path between the i-th and j-th state of H_s reads

$$P_{decay,i\to j} = \sin^2\left(\frac{\Omega_{ij}\tau}{2}\right)\frac{Q_{ij}^2}{Q_{ij}^2 + (E_j - E_i - \omega_0)^2}|\langle\Psi_i|\Psi_s\rangle|^2 \tag{4}$$

where $Q_{ij} = 2c \langle \Psi_i | A | \Psi_j \rangle$, $\Omega_{ij} = \sqrt{Q_{ij}^2 + (E_j - E_i - \omega_0)^2}$, $|\Psi_s\rangle$ is the initial state of the register qubits, $|\Psi_i\rangle$ and $|\Psi_j\rangle$ are the i-th and the $j-$th eigenvector of H_s. From Eq. (4), it is clear that the dominant resonant pathways would have a nearly perfect match between the energy gaps $(E_j - E_i)$ and ω_0. When a transition is off-resonant, i.e. $|E_j - E_i| >> \omega_0$, the corresponding contribution to the decay probability in Eq. (4) can be tuned to extremely small values in many realistic experimental set-ups. Further detail on the resonant transitions can be found in Refs. [9, 11, 12, 13] and later discussions below.

2.2 Original EC3-Solving Algorithm

We now summarize the algorithm proposed by Wang and his co-authors that exploits the resonant transition physics to perform computational tasks. Extended from the spectrum-probe algorithm in [7], EC3-solving algorithm was further designed to solve a satisfaction problem. An EC3 problem is a boolean formula F with M clauses and n binary variables $v_1, v_2, \cdots v_n$ that $F = C_1 \wedge C_2 \cdots \wedge C_M$. Each clause contains exactly three variables and it is satisfied when there is only one variable is 1 and the other two are 0. The task is to determine if there is an assignment of $v_1 v_2 \cdots v_n$ that satisfies all M clauses such that F is evaluated to 1. An energy function is defined as

$$h_i(v_1^i, v_2^i, v_3^i) = \begin{cases} 0 & \text{if } v_1^i, v_2^i, v_3^i \text{ satisfies clause } C_i; \\ 1 & \text{if } v_1^i, v_2^i, v_3^i \text{ does not satisfy clause } C_i \end{cases} \tag{5}$$

where v_z^i means the z_{th} variable in clause C_i that $z \in \{1, 2, 3\}, i \in \{1, M\}$ and $v_z^i \in \{v_1, \cdots, v_n\}$. Then it is defined that

$$H_{C_i} |v_1 v_2 \cdots v_n\rangle = h_i(v_1^i, v_2^i, v_3^i) |v_1 v_2 \cdots v_n\rangle \tag{6}$$

and

$$H_C = \sum_{i=1}^{M} H_{C_i}. \tag{7}$$

From Eq. (6)-(7), we know that for any given arbitrary assignment, H_C computes the total number of violated clauses in an EC3 instance. The state space, i.e. all the possible assignments $(N = 2^n)$, is the computational basis (also the eigen-basis) for H_C while the corresponding eigenvalue is the number of clauses violated by that eigenstate. Hence, the eigenvalues are integers in the range of 0 and M in the subspace occupied by H_C. Eigenstates with eigenvalues 0 would be the solution assignments.

The EC3-solving algorithm acts on an 1-qubit probe register R_p and one $n + 1$ qubit register R_s as shown in Figure 1. The register Hamiltonian is constructed as

$$H_s = \begin{pmatrix} -I_N & 0 \\ 0 & H_C \end{pmatrix}. \tag{8}$$

where I_N is N-dimensional identity operator. It is given that

$$A = X \otimes \left(\frac{1}{\sqrt{2}} (I_2 + X) \right)^{\otimes n} \tag{9}$$

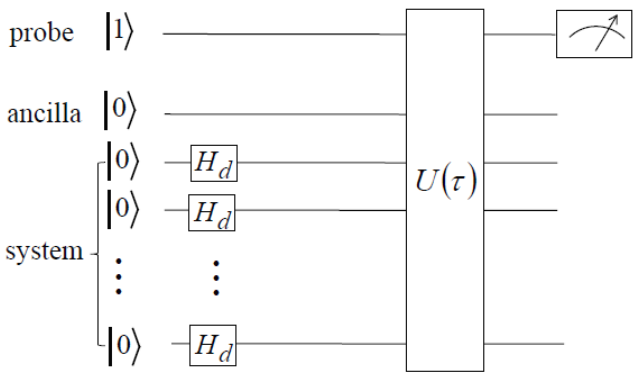

Figure 1: [8] The original EC3-solving algorithm. The register R_p has one probing qubit that is initially in the excited state. The R_s register contains $n+1$ qubits where the first qubit is an ancillary qubit while the last n qubits are the state space for all the boolean assignments. The unitary U is based on Hamiltonian H in Eq. (1) that $U = e^{-iH(\tau)}$.

and

$$|\Psi_s\rangle = (I_2 \otimes H^{\otimes n})(|0\rangle^{\otimes(n+1)}) = \frac{1}{\sqrt{N}} \sum_{j=1}^{N} |0\rangle |j-1\rangle = \frac{1}{\sqrt{N}} \sum_{j=1}^{N} |\varphi_j\rangle \tag{10}$$

From Eq. (8)-(10) we know (1) the states $|\varphi_j\rangle$ are eigenstates of H_s with eigenvalue -1 because of $-I_N$ and (2) $H_s |\Psi_s\rangle = -|\Psi_s\rangle$ where $E_s = -1$. With the additional 1 ancillary qubit in R_s, it is easier to prepare an eigenstate for H_s as $|\Psi_s\rangle$ can be prepared by using Hadamard gates on the last n_{th} qubits of register R_s. We simply set $\omega_0 = 1$ for resonance and let the system evolve for some time τ and we measure the probe qubit to see if we observe 0. If the outcome is 1, it means we have not found any solution yet. If the outcome is a 0, it means either (1) with high probability we have found the solution or (2) with low probability we obtain a non-solution state because of the error from non-solution assignments becomes non-negligible such that the energy from the probe qubit leaks to non-solution assignments.

In the RT model, a state in the cavity system climbs up from eigen state $|\Psi_i\rangle$ to state $|\Psi_{i+1}\rangle$ by using the energy given from the probe qubit when the eigen energy gap $E_{i+1} - E_i$ is equal to the frequency ω_0 . In this setting, we know the state $|\Psi_s\rangle$ can be also viewed as state $|\Psi_0\rangle$ because $E_s = E_0 = -1$ as $E_1 = 0$. The evolution of $|\Psi_0\rangle$ to all other states, solution assignment(s) state $|\Psi_1\rangle$ and non-solution assignments $|\Psi_j\rangle$, will contribute to the probability of observing a 0 in register R_p. It is clear to see that each $|\Psi_j\rangle$ state is associated with eigen energy E_j and it can be expressed as

$$|\Psi_j\rangle = \sum_{l=1}^{m_j} \frac{1}{\sqrt{m_j}} |1\rangle |\mu_l\rangle \tag{11}$$

where m_j is the number of eigenstates associated with eigenvalue E_j and $|1\rangle |\mu_l\rangle$ is the corresponding eigenstate. The contribution from the solutions states (states with eigenvalue 0) is

$$P_{decay} = \sin^2(\frac{\Omega_{01}\tau}{2}) \tag{12}$$

The contribution from all non-solution states is [8]

$$P_{decay}^{err} = \sum_{j=2}^{N} \sin^2(\frac{\Omega_{0j}\tau}{2}) \frac{Q_{0j}^2}{Q_{0j}^2 + E_j^2}{}^1. \tag{13}$$

Since $Q_{ij} = 2c \langle \Psi_i | A | \Psi_j \rangle$ and we know that

$$\begin{aligned} \langle \Psi_0 | A | \Psi_j \rangle &= \frac{1}{\sqrt{N}} \frac{1}{\sqrt{m_j}} \sum_{j=1}^{N} \sum_{l=1}^{m_j} \left((\langle 0 | \langle j |) A \right) |1\rangle |\mu_l\rangle \big) \\ &= \frac{1}{\sqrt{N}} \frac{1}{\sqrt{m_j}} \sum_{j=1}^{N} \sum_{l=1}^{m_j} \big(\langle 1 | \sum_{k_j=0}^{N-1} \frac{1}{\sqrt{N}} \langle k_j | \big)(|1\rangle |\mu_l\rangle \big) \\ &= \frac{1}{N} \frac{m_j}{\sqrt{m_j}} \sum_{j=1}^{N} 1 \\ &= \sqrt{m_j}. \end{aligned} \tag{14}$$

Q_{0j} is therefore $2c\sqrt{m_j}$ where m_j is the degeneracy of the assignments (basis states) of H_C with eigenvalue E_j. The upper bound of decay error probability P_{decay}^{err} can be simplified to

$$P_{decay}^{err} \leq \sum_j \frac{Q_{0j}^2}{{Q_{0j}}^2 + {E_j}^2} \leq \sum_j \frac{4c^2 m_j}{{E_j}^2} \leq \frac{2}{3}\pi^2 c^2 m_{max}, \tag{15}$$

where m_{max} is the maximum of m_j, given the fact that $\sum_{j=2}^{\infty} \frac{1}{(j'-1)^2} = \frac{\pi^2}{6}$. We have to choose the coupling factor $c \simeq O(\frac{1}{\sqrt{m_{max}}})$ to make P_{decay}^{err} become negligible. However, this imposes the dilemma. If we have a huge degeneracy (exponentially large) in the system, then we need to set τ to be exponentially large ($\tau \simeq \frac{1}{c}$) for *each iteration* since

$$P_{decay} = \sin^2(c\sqrt{m_0}\tau) \tag{16}$$

has to be some non-negligible number. If τ is some constant number, then P_{decay} will be exponentially small. That makes the number of required iterations ($\Delta \simeq \frac{1}{P_{decay}}$) exponential large and the overall complexity $\Delta \times \tau$ would be huge. Furthermore, for hard instances of solvable satisfaction problems, m_0 is a small number as it is the number of satisfying assignments. When we observe a 0 in the probe qubit, it implies that with high probability the solution state is obtained. Hence, we will examine the potential issues based on (1) decay error probability and (2) energy leak due to high degeneracy.

We remark that our analyses above restricts to Hamiltonians for EC-3 or 3-SAT problems encoded with specific energy functions which assign the (integer-valued) energies according to the number of clauses violated. For more general Hamiltonians, the success probability of the algorithm depends on more factors as discussed in Ref. [14].

[1] in this case, the initial state $|\Psi_s\rangle$ is also the eigenstate of H_s with eigenvalue -1 such that $|\Psi_s\rangle$ that will be excited to other eigenstates with higher eigenvalues.

2.3 Physical Implementation

We next clarify the physical implementations of the full Hamiltonian H in terms of elementary Pauli matrices for qubits. First, we define the projection operator

$$Z^+ = |0\rangle\langle 0| = \frac{1}{2}(\mathbb{I} + \sigma_z), \qquad Z^- = |1\rangle\langle 1| = \frac{1}{2}(\mathbb{I} - \sigma_z).$$

Each energy function in h_i in Eq. (5) can now be straightforwardly translated into a linear combination of three-qubit projections,

$$\begin{aligned} h_i(v_1^i, v_2^i, v_3^i) &= \big(\mathbb{I} - \left|0_{v_1^i} 0_{v_2^i} 1_{v_3^i}\right\rangle\left\langle 0_{v_1^i} 0_{v_2^i} 1_{v_3^i}\right| - \left|0_{v_1^i} 1_{v_2^i} 0_{v_3^i}\right\rangle\left\langle 0_{v_1^i} 1_{v_2^i} 0_{v_3^i}\right| - \left|1_{v_1^i} 0_{v_2^i} 0_{v_3^i}\right\rangle\left\langle 1_{v_1^i} 0_{v_2^i} 0_{v_3^i}\right|\big) \\ &= \Big(\mathbb{I} - Z_1^+ Z_2^+ Z_3^- - Z_1^+ Z_2^- Z_3^+ - Z_1^- Z_2^+ Z_3^+\Big). \end{aligned} \tag{17}$$

We then expand the projection operators using Pauli matrix Z, for instance,

$$Z_1^+ Z_2^+ Z_3^- = \frac{1}{8}\Big(\mathbb{I} + \underbrace{Z^1 + Z^2 + Z^3}_{\text{one body}} + \underbrace{Z^1 Z^2 - Z^1 Z^3 - Z^2 Z^3}_{\text{two body}} - \underbrace{Z^1 Z^2 Z^3}_{\text{three body}}\Big).$$

The full register Hamiltonian (coupling the n-register qubits to the ancillary one) can also be re-written in terms of the projection operators introduced earlier,

$$H_s = -Z_0^+ \otimes I + Z_0^- \otimes H_c$$

where Z_0^- and Z_0^+ act on the ancillary qubit. As for the register-probe interaction, the operator A given in Eq. (9) is already fully specified in terms of Pauli matrices.

It is now clear that the EC3 problems require building intricate many-body interactions among qubits in the present framework. While the two-body interaction can be generated easily in most cavity-related quantum optical experiments, a major challenge is to coherently couple multiple (beyond 2) register qubits that might not be in a close vicinity of each other. This obstacle prevents implementing the present algorithm in a large scale experiment involving many register qubits at the moment. Nevertheless, with the recent progress of various quantum technologies such as the quantum bus[18] and the many-body Hamiltonian simulations [15, 16, 17], the future prospect of constructing the required multiple-qubit interacting Hamiltonian is certainly promising. This could be particularly true as the present framework only requires static (alway-on) interactions as opposed to time-dependent (on-demand) interactions among the qubits. This static requirement is true for both the energy functions, h_i, as well as for register-probe interaction, H_{int}.

3 Comparison to Adiabatic Quantum Computation

We now analyze the intimate connections between RT and AQC models. First, we briefly summarize the essence of AQC [5] to make the analysis in this work self-contained.

Based on the adiabatic theorem [19], a quantum system evolves according to Schrödinger equation

$$i\frac{d}{dt}|\psi(t)\rangle = H_c(t)\,|\psi(t)\rangle\,, \tag{18}$$

we can consider a family of Hamiltonians $\tilde{H}(s)$, $0 \leq s \leq 1$ and let $H(t) = \tilde{H}(t/T)$. Define the instantaneous eigenstates and eigenvalues

$$H(s)\,|l;s\rangle = E_l(s)\,|l:s\rangle \tag{19}$$

where

$$E_0(s) \leq E_1(s) \leq \cdots \leq E_{N-1}(s) \tag{20}$$

and the minimum spectral gap is

$$g_{min} = \min_{0\leq s\leq 1}(E_1(s) - E_0(s)). \tag{21}$$

It is well-known that the expected running time

$$T \gg \frac{\epsilon}{g_{min}^2} \quad s.t. \quad \langle l=0; s=1|\psi(T)\rangle \simeq 1. \tag{22}$$

where

$$\epsilon = max_{0\leq s\leq 1}|\langle l=1;s|\frac{dH}{ds}|l=0;s\rangle|. \tag{23}$$

This concept was further extended [5] in a linear manner. The computation starts by initializing the AQC in the easy-to-prepare ground state(s) of the Hamiltonian H_B. The time dependent Hamiltonian $H(t)$ is defined as

$$H(t) = (1-s)H_B + sH_C \tag{24}$$

where $s = f(t/T)$. In this study, we consider $s = t/T$ for simplicity. We simply let the ground state of H_B evolve in this Hamilton $H(t)$. When $t = T$, the ground state $|l=0;s=0\rangle$ of H_B will evolve into state $|\psi(t)\rangle$ that is extremely close to the ground state $|l=0;s=1\rangle$ of H_C. The running time of AQC is determined by the minimal spectral gap g_{min} of the underlying Hamiltonians [5].

In the following three subsections, we shall investigate (1) how to adapt any AQC algorithm to a corresponding RT version to firmly establish their connections as computational devices, (2) how the performance of RT and AQC model differs in different computational problems due to the very different physical mechanism by which the models operate, and (3) how to interpret the underlying quantum dynamics of RT model in terms of well-established and well-studied AQC models.

3.1 Translation of Algorithms

Figure 2 presents a clear picture of how the two computational models are related. In both models, the solution to a computational problem is encoded in the ground state of a Hamiltonian H_C. If it is easy to initialize a quantum device in the ground state of H_C then the problem is directly solved without invoking either AQC or RT models. Hence, both AQC and RT models are initialized with an easy-to-prepare quantum state and rely on different physical principles (adiabatic theorem versus resonant transition) to manipulate the quantum dynamics in order to achieve the desired ground state of H_C.

As described earlier and shown in the figure, the AQC model would initialize the device in the ground state of another Hamiltonian H_B, which is related to H_C via a simple linear equation as in Eq. (24). As long as this transformation of Hamiltonians (from H_B to H_C) is adiabatically slow, the quantum device remains in the instantaneous ground state of the time-evolved Hamiltonian. This guarantees the attainment of the ground state of H_C at the end of the algorithm execution.

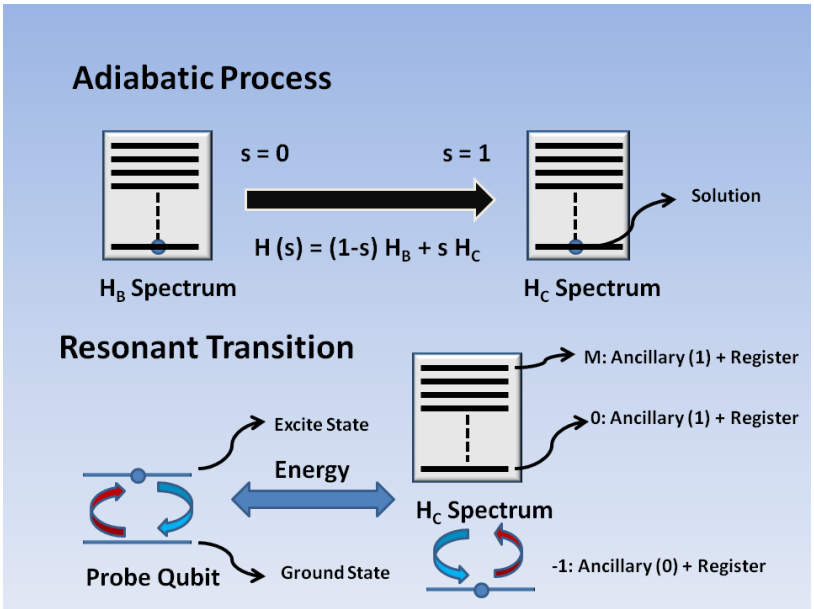

Figure 2: Connections between AQC and RT. In both models, the desired solution is encoded as the ground state of H_C. In the RT model, the H_C is embedded into a larger Hamiltonian after introducing the ancillary qubit. The enlarged system is then excited from the -1-eigenvalue manifold to the 0-eigenvalue manifold with the help of the probe qubit. On the other hand, the AQC model starts with H_B (easy to initialize in the ground state) and relies on adiabatic tuning to morph to Hamiltonian to H_C.

On the other hand, the RT model would add an ancillary qubit to the system (with Hamiltonian H_C) to define an extended Hamiltonian for the enlarged system. For instance, this is how the register Hamiltonian H_s, Eq. (8), for the EC3 solving algorithm is defined earlier. As shown, the desired Hamiltonian H_C appears at the lower diagonal part of the enlarged Hamiltonian in Eq. (8). We note that H_s Hamiltonian essentially introduces a highly degenerate ground state and the rest of the spectral properties of H_s is determined by H_C Hamiltonian. It would be easy to initialize the enlarged system in the ground state with eigenvalue -1 since this is determined solely by the ancillary qubit's quantum state. By properly tuning the probe qubit's energy to target the transition between the -1 and 0 eigenvalue manifold of this extended system, the desired state (ground state of H_C) can also be reached reliably.

Hence, the translation of adiabatic algorithms is now clear. One simply takes H_C (the final Hamiltonian in an adiabatic algorithm) and embedded into H_s as done in Eq. (24). This straightforward mapping establishes the RT model potentially being a universal quantum computation framework.

3.2 Different Limiting Factors

We now compare the performance of AQC model and RT model when attacking two types of problems: Minimum Hamming Weight Problem and Perturbed Minimum Hamming Weight Problem. A Minimum Hamming Weight problem (MHWP) is that for a given n bit string $z \in \{0,1\}^n$, we want to minimize the Hamming weight $w(z)$ of z. In the MHWP problem, it is shown that the

complexity is $O(1)$ for AQC [6]. If we look at the final Hamiltonian H_C, we know that many eigenstates (in the computational basis) would have the same eigenvalues. For instance, when $n = 3$, binary strings 011, 101 and 110 have the same Hamming weight. When eigenvalue $e_{n/2} = \frac{n}{2}$, we have $C(n, n/2)$ eigenstates, which is approximately $O(2^n/n^2)$ by Stirling's approximation. That is the the corresponding maximum degeneracy of the system. Hence, the RT model would have a complexity of $O(\sqrt{\frac{2^n}{n^2}})$ when it is easy to prepare the initial state with eigenvalue ω_0 shifted from the eigenvalue of the all zeros string. It is clear in this case that AQC performs much better than RT based models in the simple MHWP problem.

In a Perturbed Miminum Hamming Weight Problem (PMHWP), a Hamiltonian of the system is expressed as

$$H_f(t) = H(t) - \frac{t}{T}(n+1)\left|1^n\right\rangle\left\langle 1^n\right| \tag{25}$$

and it is shown [6] that for the Hamiltonian H_f : $g_{min} \in O(\frac{n}{\sqrt{2^n}})$ and this implies $T \gg \Omega(\frac{2^n}{n^2})$. Similarly, for the RT model, the complexity for PMHWP remains $O(\sqrt{\frac{2^n}{n^2}})$ exactly the same as that for MWHP since small perturbation from $\left|1^n\right\rangle\left\langle 1^n\right|$ does not affect where the most degeneracy occurs and does not change the degree of highest degeneracy. The perturbation will only affect (decrease or increase) the degeneracy of eigenstate $|1\rangle^{\otimes n}$ by at most n, which is significantly smaller than $C(n, n/2)$. In such a scenario, small perturbation, the RT model is almost perturbation blind and outperforms AQC.

Hence, when solving the eigenstate/eigenvalue problems (such as CSP, MHW, and search), we need to examine the nature of the problem in order to choose the right model. From a very intuitive sense, we can imagine that RT model and AQC model are similar but their running time is dominated by different parameters. In the AQC model, the running time is dominated by the inverse of the square of the minimal spectral gap $1/g_{min}^2$ while in the RT model, the running time is dominated by the square root of the maximal degeneracy $\sqrt{m_{max}}$.

Finally, we emphasize that the above comparisons are based on idealistic situations in which no noise or decoherence is considered. In the study of resonant transitions physics, it is well known that a signficant quantum state leakage into high-lying energy state is highly unlikely due to the violation of energy conservations . In fact, if this type of quantum leakage happened all the time, it would have completely altered the robust resonant transition physics observed ubiquitously. This being said, temporary virtual transition into the high-lying energy states then back down to the resonant states can happen as allowed by the Heisenberg's time-energy uncertainty principle. Hence, the realistic problem is not really the leakage problem but rather the dephasing problem. As the qubits temporarily change their states, important quantum phase information will be lost. Fortunately, the phase factors of a wave function is not explicitly used in the RT model. This allows the RT model, similar to the AQC model, to be more *noise-resilient* than the traditional circuit models where the computational time has to be significantly less than the single qubit's dephasing time, for instance.

3.3 Adiabatic Evolution Following Resonant Transition Model

To complete the analysis, now we would like to compare the underlying quantum dynamics of the two models and gain a different perspective on their connections. We follow closely a method of

analysis presented by Wong and Myer [20] in which one can make AQC to emulate other unitary dynamics based quantum computation models. The idea is to project complicated many-qubit quantum dynamics into the dynamics of an effective qubit. One then asks how to engineer an appropriate adiabatic path for this effective qubit's Hamiltonian such that the time evolved ground state emulates the dynamical evolution in another system. Being an effective two-state description, one can view the adiabatic ground state evolutions as a trajectory on the Bloch sphere.

Through these simplified representations, Wong and Myer provide an illuminating account of the subtle differences between AQC and continuous quantum walk (CQW) model, another universal quantum computation paradigm based on the unitary quantum dynamics. In Ref. [20], it was shown that for AQC to emulate the quantum walk search algorithm, it must interpolate between three fixed Hamiltonians ($\tilde{H}_B, \tilde{H}_E, \tilde{H}_C$). That implies in order to emulate the behavior of a quantum walk via the use of AQC, the corresponding Hamiltonian for AQC is structurally beyond a linear interpolation between the initial Hamiltonian, $\tilde{H}_B$, and the final Hamiltonian, $\tilde{H}_C$. Not surprisingly, adopting the same projected representation, we find the AQC can more naturally emulate the RT model; although with an *unusual adiabatic path*.

To make AQC emulate RT model in the approach just described above, let us first formulate the RT model in this two-state description. We first focus on the system part and exclude the ancillary and probe qubits. The solutions of a computational problem are designated as one quantum state $|g\rangle$ and every other states are denoted as $|i\rangle$. Next we incorporate the probe and ancillary qubits into the two-state description. We now define augmented basis with $|G\rangle = |01g\rangle$ and $|B\rangle = |10b\rangle$ with $|b\rangle = \sum_{i=0}^{2^n-1} \frac{1}{\sqrt{2^n}} |i\rangle$ where the three indices of the kets denotes the state of the probe qubit, the ancillary qubit and the cavity system, respectively. In this augmented basis, we can now depict the time evolution of the entire quantum device in which an initial state $|\Psi_0\rangle = |B\rangle$ is time evolved under the unitary operation, $U = e^{-iH\tau}$. The time evolution of $|\Psi_0\rangle$ can be expressed as

$$|\Psi_0(\tau)\rangle = \sqrt{P_{decay}}\,|01g\rangle + \sqrt{1-P_{decay}}\,|10b\rangle = \alpha(\tau)\,|G\rangle + \beta(\tau)\,|B\rangle \tag{26}$$

where H is described in Eq. 1. In this case we obtain

$$\Omega_{0,1} = 2c, \quad P_{decay} = \sin^2(\frac{\Omega_{0,1}\tau}{2}) = \sin^2(c\tau) \tag{27}$$

by the result from Eq. 4, 14 and 16 and assuming there is only one solution. Then we want the ground state of the adiabatic Hamiltonian $H_A(\tau)$ to be $|\Psi_0(\tau)\rangle$ with eigenvalue λ_0. The other eigenstate is hence

$$\left|\Psi_0{}^{\perp}(\tau)\right\rangle = \beta(\tau)\,|G\rangle - \alpha^*(\tau)\,|B\rangle \tag{28}$$

with eigenvalue $\lambda_0^{\perp}$. Similar to the analysis by Wong and Meyer, to avoid complex number, in [20] with eigenvalues $\lambda_0 = -\lambda_0^{\perp}$, the Hamiltonian is

$$\begin{aligned}
\tilde{H}_A(\tau) &= \lambda_0\,|\Psi_0(\tau)\rangle\langle\Psi_0(\tau)| + \lambda_0^{\perp}\left|\Psi_0^{\perp}(\tau)\right\rangle\left\langle\Psi_0^{\perp}(\tau)\right| && (29)\\
&= \lambda_0^{\perp}\begin{pmatrix} -|\alpha|^2+\beta^2 & -2\alpha\beta \\ -2\alpha^*\beta & |\alpha|^2-\beta^2 \end{pmatrix} && (30)\\
&= \lambda_0^{\perp}\begin{pmatrix} -\sin^2(c\tau)+\cos^2(c\tau) & -2\sin(c\tau)\cos(c\tau) \\ -2\sin(c\tau)\cos(c\tau) & \sin^2(c\tau)-\cos^2(c\tau) \end{pmatrix} && (31)\\
& && (32)
\end{aligned}$$

The Hamiltonian is thus reduced to

$$\tilde{H}_A(s) = \lambda_0^{\perp}(s)[-(1-2s)\tilde{H}_C + \sqrt{s(1-s)}\tilde{H}_E] \tag{33}$$

where

$$s(t) = \sin^2(c\tau) \tag{34}$$

is the interpolation schedule and we have

$$\tilde{H}_C = \begin{pmatrix} -1 & 0 \\ 0 & 1 \end{pmatrix}, \qquad \tilde{H}_E = \begin{pmatrix} 0 & -2 \\ -2 & 0 \end{pmatrix}. \tag{35}$$

We still need to find out $\lambda_0^{\perp}$ in terms of s. By use of the adiabatic theorem $ds/dt = \epsilon g^2(s)$ and Eq. (34), we have

$$2\sin(c\tau)\cos(c\tau)c = \epsilon g^2(s). \tag{36}$$

Since $\lambda_0 = -\lambda_0^{\perp}$, i.e. $\lambda_0^{\perp} = g(s)/2$, then we obtain

$$g(s) = \sqrt{\frac{2c\sqrt{s(1-s)}}{\epsilon}}, \quad \lambda_0^{\perp} = \sqrt[4]{\frac{c^2 s(1-s)}{4\epsilon^2}}. \tag{37}$$

Therefore, the adiabatic Hamiltonian that follows the evolution in a RT-based algorithm is

$$\tilde{H}_A(s) = \sqrt[4]{\frac{c^2 s(1-s)}{4\epsilon^2}}[-(1-2s)\tilde{H}_C + \sqrt{s(1-s)}\tilde{H}_E]. \tag{38}$$

Unlike the case presented in Ref. [20], the AQC emulates the RT dynamics via a non-linear and closed adiabatic path which starts with $-\tilde{H}_C$ at $s = 0$ and returns to $\tilde{H}_C$ at $s = 1$. Note the sign difference in the beginning and the end of the adiabatic path.

The initial input to the system is $|10b\rangle$ and is also the ground state of -$\tilde{H}_C$. This points to a fundamental difference between RT and AQC models. In the AQC case, one would like to initialize the quantum device into the ground state of $\tilde{H}_B$, which should preferably overlap significantly with the desired output state as much as possible and limit the need to perform the adiabatic transitions. In the RT model, we actually want the initial state to be completely orthogonal to the desired state because the resonant transitions imply a jump from one eigenstate to another. In the two-state description, this would imply the initial state has to be $|B\rangle$ (completely orthogonal to $|G\rangle$). This physical circumstances explain the unusual closed adiabatic path AQC must follow in order to emulate the RT model.

In this two-state projected view, it is also clear that the RT dynamics is different from that of the CQW consider in Ref. [20]. For instance, the Hamiltonian $\tilde{H}_e$ acts more powerfully than the standard oracular operations. Unlike a standard oracular operation which first reflects around $|G\rangle$ by applying a phase then reflects around the initial state, the Hamiltonian $\tilde{H}_e$ introduces an extra structure that drives the evolution between $|G\rangle$ and $|B\rangle$.

4 3-SAT Problems

To further illustrate the usefulness of RT-based quantum computations, we generalize the EC3 algorithm presented earlier to study hard instances in 3-SAT problems. Through this highly non-trivial problem, we will address how to improve the efficiency of a RT model. We recall a 3-SAT

is defined as a formula F with M clauses and n binary variables. Let $N = 2^n$ be the number of possible assignments for n boolean variables. Let $V = \{v_1, v_2, \cdots, v_n\}$ be the set of boolean variables and $\bar{V} = \{\bar{v}_1, \bar{v}_2, \cdots, \bar{v}_n\}$ be the complement set. A 3-SAT formula is described as

$$F = C_1 \wedge C_2 \wedge \cdots \wedge C_M \quad and \quad C_i = (l_1^i \vee l_2^i \vee l_3^i)$$

where (1) $\forall i \in \{1, M\}$, literal $l_j^i \in V$ or literal $l_j^i \in \bar{V}$ and (2) $\forall k \in \{1, n\}$, v_k or $\bar{v}_k$ appears at least once in F. The task is to find an assignment to $v_1, v_2, \cdots, v_n$ such that F will be evaluated to 1.

4.1 RT algorithm

Given a 3-SAT formula F, we associate each 3-bit clause with an energy function, modified from Eq. (5),

$$h_i(C_i) = h_i(l_1^i, l_2^i, l_3^i) = \begin{cases} 0 & \text{if } l_1^i, l_2^i, l_3^i \text{ satisfies clause } C_i; \\ 1 & \text{if } l_1^i, l_2^i, l_3^i \text{ does not satisfy clause } C_i, \end{cases} \tag{39}$$

where l_z^i is the z_{th} literal in clause C_i. We can consider this energy function as a *constant energy function*. Similarly, we can also have the clause associated with another energy function

$$h_i(C_i) = h_i(l_1^i, l_2^i, l_3^i) = \begin{cases} 0 & \text{if } l_1^i, l_2^i, l_3^i \text{ satisfies clause } C_i; \\ \gamma \times i & \text{if } l_1^i, l_2^i, l_3^i \text{ does not satisfy clause } C_i, \end{cases} \tag{40}$$

we can consider this second energy function as *clause dependent energy function*. With both energy functions, each local Hamiltonian H_{C_i} can be defined by its action on quantum state vectors,

$$H_{C_i} |v_1 v_2 \cdots v_n\rangle = h_i(l_1^i, l_2^i, l_3^i) |v_1 v_2 \cdots v_n\rangle . \tag{41}$$

Hence, the Hamiltonian $H_C = \sum_i H_{C_i}$ gives an energetic value to each configurations of all qubits according to which clauses C_i are violated. The solutions to a 3-SAT problem would correspond to the zero-energy eigenstates of H_C if they exist. Similar to the EC3 algorithm introduced earlier, one needs to introduce an additional ancillary qubit and embed H_C within the extend structure of Hamiltonian H_s as done in Eq. (8). Details of how to construct all these abstract Hamiltonians in terms of Pauli matrices can be inferred from Sec. 2.3.

To improve performance of RT-based quantum computation, it is desirable to reduce the decay error probability P_{decay}^{err} described in Eq. (15). Intuitively, we can either (1) increase the eigenvalue gap (detuning effect) to suppress the decay error probability P_{decay}^{err} and (2) increase the number of distinct eigenvalues in the spectrum of H_C to minimize the degeneracy in each eigenenergy manifold. These two objectives can be simultaneously achieved through the modifications introduced in Eq. (40).

4.2 3-SAT Hard Instances

It is well-known that, in general, the difficulty of a 3-SAT problem is gauged by an order parameter known as the clause-variable ratio, (M/n). When the ratio is around $M/n \simeq 4.24$, then the problem can undergo a phase transition[21, 22, 23, 24] and be classified as NP-complete. When the order parameter is significantly different from the critical value of 4.24, then the problem becomes relatively trivial. Next we use either Eq. (39) or Eq. (40) as the energy function required by the 3-SAT algorithm presented in Sec. 4.1 and compare the performance of the corresponding algorithm in a hard instance of the 3-SAT problem.

4.2.1 Constant Energy Function

In this subsection, we will analyze RT-based algorithm to solve a hard 3-SAT instance. We will take a constant energy function, based on Eq. (39), that assigns a numerical value 1 whenever a clause is violated. Given the constraint from a hard 3-SAT instance, the decay probability error can be bounded from above with respect to M. We obtain [2] a new upper bound

$$P_{decay}^{err} \leq \sum_j \frac{4c^2 m_j}{{E_j}^2} \leq 4c^2 m_{max} \sum_{j'=1}^{j'=4n} \frac{1}{{j'}^2} \leq 4c^2 (\frac{\pi^2}{6} - \frac{2M-1}{2M^2}) m_{max}. \tag{42}$$

Regarding the performance, the main concern is the maximal degeneracy m_{max}. With $M+1$ eigenvalues and N eigenstates, even distributed uniformly, each eigenvalue has an expected exponential $\mathrm{O}(\frac{N}{4n})$ degree of degeneracy. It is inevitable that m_{max} is *exponentially* large for 3-SAT hard instances, given the constructed H_C based on Eq. (39). This implies the coupling factor c (between the register and the probe) has to be exponentially small in order to make P_{decay}^{err} negligible. This ultra-weak coupling is, however, not a desired solution as the running time τ will necessarily scale to an exponentially large quantity, $(O(\sqrt{m_{max}}))$, as summarized in Table 1. The worst case is that there is only one solution assignment and all the degeneracy occurs at the non-solution assignments that only violate one clause. In such a scenario, the complexity of the RT approach is $O(\sqrt{N})$.

Method	**Running time**	**time unit**
RT with Constant Energy Function	$O(\sqrt{m_{max}})$	Continuous Time
Conventional Grover	$O(\sqrt{2^n})$	Discrete, Oracle Invocations

Table 1: Time complexity for two types of quantum algorithms for solving SAT.

For conventional discrete quantum search algorithms, such as Grover's search algorithm on unstructured data [**?**], the complexity is $O(\sqrt{N})$ when there are only a few solutions. Let us consider a uniform situation that the given $2^n - 1$ non-solution assignments will be *evenly distributed* among one eigenvalue, two eigenvalues and so on till M eigenvalues. *On the average*, in comparison to conventional discrete quantum search algorithms, the RT algorithm outperforms the conventional quantum search algorithms in hard instances since the expected running time of each iteration is [3]

$$\mathbb{E}(\tau) \simeq \mathbb{E}(\frac{1}{c}) \simeq \mathbb{E}(\sqrt{m_{max}}) = \frac{\sum_{i=1}^{M} \sqrt{\frac{N}{i}}}{M} \simeq O(\sqrt{N/n}) \tag{43}$$

4.2.2 Clause Dependent Energy Function

Now we will adapt the modified energy function introduced in Eq. (40). From Eq. (15), it is shown that $P_{decay}^{err} \leq \sum_j \frac{4c^2 m_j}{{E_j}^2}$. In the worst case scenario, we have only one solution and each of the the rest of $2^n - 1$ assignments violates only one clause (the first clause). Given such a condition, we

[2] On Mathematica, harmonicnumber(M,2), is bounded from above by $\frac{\pi^2}{6} - \frac{2M-1}{2M^2}$ by use of Laurent series

[3] On Mathematica, harmonicnumber(M,1/2)/M, is approximately $2\sqrt{\frac{1}{M}}$ by Puiseux series

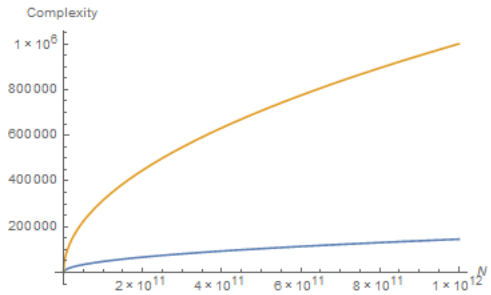

Figure 3: Top line for the conventional discrete quantum search algorithm, the bottom line is for spectra probing algorithm. The x axis is the number of possible assignments (N) in hard cases in a constraint satisfaction problem F. The y axis is the complexity.

have

$$P_{decay}^{err} \leq \frac{4c^2(N-1)}{(\gamma)^2}. \tag{44}$$

Since the running time τ of each iteration is proportional to the inverse of coupling factor c, i.e.

$$\tau \simeq \frac{1}{c}, \tag{45}$$

and we have to make the P_{decay}^{err} a relatively small constant, then we know $\tau \simeq O(\frac{\sqrt{N}}{\gamma})$. It is clear that γ defined in Eq. (40) improves the running time of the adapted algorithm as γ gets larger. Suppose γ is a positive integer, i.e. $\gamma \in [1, 2, \cdots, \infty]$ and the cost of increasing γ is constant, then the rate of improvement remains positive but monotonically drops as γ is scaled up. When $\gamma \propto \sqrt{N}$, the running time τ would approach a plateau value independent of input size. Unfortunately, the ideal scenario is difficult to attain as it is unrealistic to scale γ arbitrarily large in experiments. The benefit of having a large γ is physically intuitive and reflects in improved algorithmic performances.

Regarding the average case, for the simplicity of the analysis, let us assume the distribution of the non-solution assignments to corresponding eigenvalues is uniform. Given $2^n - 1$ non-solution assignments, they will be *evenly distributed* among one eigenvalue, two eigenvalues and so on till $\frac{M(M+1)}{2}$ eigenvalues. In each case, we will have m_{max} equal to 2^n, $2^n/2, 2^n/3 \cdots$ and $2^n/(M(M+1)/2)$, respectively. We derive [4]

$$\mathbb{E}(\tau) \simeq \mathbb{E}(\frac{\sqrt{m_{max}}}{\gamma}) = \frac{1}{\gamma}\frac{\sum_{i=1}^{K}\sqrt{\frac{N}{i}}}{K} \simeq O(\sqrt{N}/(n\gamma)) \tag{46}$$

where $K = (M(M+1))/2$. In comparison to the performance of the solver that adapts the constant energy function as shown in Eq. (43), we notice that the algorithm that adapts the clause dependent energy function outperforms by a factor of γ and $\sqrt{n}$. The improvement is two-fold in the solver that adapts clause dependent energy function. The first improvement comes from the variable γ that we can control in the experiment. The second improvement, the factor $\sqrt{n}$, comes from the

[4] On Mathematica, (harmonicnumber $((M*(M+1)/2), 1/2))/M$ converges around 1.5. Since $K = \frac{M(M+1)}{2}$, then $O(\frac{2\times 1.5\sqrt{N}}{\gamma(M+1)}) \simeq O(\sqrt{N}/(n\gamma))$.

fact that, being clause dependent in the energy function, we broaden the bandwidth of the spectrum (from M to $\frac{M\times(M+1)}{2}$) while the number of underlying eigenstates remains as N. A wider spectrum of eigenvalues leads to a lower number of the expected maximal degeneracy.

5 Discussion

In this work, we critically analyze a novel quantum computational paradigm which encodes solution of a computational problem in eigenstates of a Hamiltonian and invoke the trick of resonant transition to explore these eigenstates. Our main focus is to fully understand how the RT model compares and contrasts with the well-established and highly related AQC model. To this end, we provide a straightforward scheme to translate any AQC algorithm into a corresponding RT version. We also briefly comment on how to build up the extended Hamiltonian for the entire system (register qubits, ancillary qubit and probe qubit) in terms of elementary Pauli matrices.

To further understand the subtle differences in the underlying quantum dynamics driving both computational models, we use simple Hamming weight problems [6] to distinguish the influences of different spectral properties of the Hamiltonian on the computational performances. In AQC, the spectral gap size determine how fast the adiabatic execution of an algorithm can take place. In RT model, for Hamiltonians based on the constant energy functions, it is the degeneracy structure of the Hamiltonian's eigen-spectrum that determine the execution speed. Through the toy model analyses, we argue that certain AQC algorithms will be more efficiently implemented in a RT model. Since both computational models rely on complicated many-body quantum dynamics to proceed, it would be illuminating to compare these underlying dynamics in some simple fashion. In this study, we adopt Wong's method that depicts the entire computational procedure as an effective qubit starting from some initial state and gradually moves toward the target (solution) state on a Bloch sphere. In this simplified view, we find RT dynamics follows a very different path than the AQC model on the Bloch sphere. In conclusion, while our algorithmic translation scheme might deceptively convey the impression that both models are almost identical at a conceptual level, the detailed dynamical analyses reveal the irreconcilable differences between the two under the hood.

Our second focus is to assess straightforward approaches one can take to fine tune the performance of an RT model in a highly non-trivial algorithmic context. In particular, we choose to illustrate these points by generalizing the original EC3-solving algorithm[8] to consider the infamous 3-SAT problem. Through this NP-complete example, we demonstrate an enhanced performance of the RT model by adopting a modified energy function in Sec. 4.2.2 that reduces the degeneracy structure of the Hamiltonian's spectrum and suppresses decay errors due to off-resonant transitions. In Table 2, the time complexity of RT algorithms based on the two different energy functions is summarized.

Method	**Worst Case**	**Average Case**
Costant Energy Function	$O(\sqrt{N})$	$O(\sqrt{\frac{N}{n}})$
Clause Dependent Energy Function	$O(\sqrt{N}/\gamma)$	$O(\sqrt{N}/n\gamma)$

Table 2: Time complexity for the two energy functions.

In summary, we find an RT model to be a convenient and practical alternative to AQC in certain contexts. A simple criterion to decide which model to use is to compare the running time, which

can be deduced from the spectral gap size of adiabatically connected Hamiltonians and the spectral degeneracies of the target Hamiltonian. The fact that one does not have to design an entirely new algorithm for the RT model should be a particularly desirable trait. For instance, the EC3 and 3-SAT algorithms presented above are clearly adapted from the original adiabatic versions. Similar to the efforts to introduce ultra-fast adiabatic process in the adiabatic computing community, there are potential ways to further enhance the physics of resonant transitions[25, 26, 27], such as exploiting the additional quantum effects when multiple probe qubits are introduced.

6 Acknowledgments

C. C. gratefully acknowledges the support from the State University of New York Polytechnic Institute.

References

[1] D. Deutsch and R. Jozsa *Rapid solutions of problems by quantum computation*, Proceedings of the Royal Society of London A 439, 1992

[2] P. Shor, *Algorithms for quantum computation: discrete logarithms and factoring*, Proceedings of the 35th IEEE Symposium on Foundations of Computer Science. pages 124-134, 1994

[3] V. Denchev, S. Boixo, S. Isakov, N. Ding, R. Babbush, V. Smelyanskiy, J. Martinis, and H. Neven, *What is the computational value of finite range tunneling*, arXiv:1512.02206 [quant-ph]

[4] E. Crosson and A. Harrow, *Simulated quantum annealing can be exponentially faster than classical simulated annealing*, arXiv:1601.03030 [quant-ph]

[5] E. Farhi, J. Goldston, S. Gutmann and M.Sipser, *Quantum computation by adiabatic evolution*, MIT-CTP-2936, 2000

[6] V. Dam, M. Mosca and U. Vazirani, *How powerful is adiabatic quantum computation*, FOCS '01 Proceedings of the 42nd IEEE symposium on Foundations of Computer Science, pp. 279 - 287, 2001

[7] H. Wang, S. Ashhab, and F. Nori, *Quantum algorithm for obtaining the energy spectrum of a physical system*, Phys. Rev. A 85.062304, 2012

[8] H. Wang, H. Fan, and F. Li, *A quantum algorithm for solving some discrete mathematical problems by probing their energy spectra*, Phys Rev. A 89.012306, 2013

[9] N. Wiebe, D. Berry, P. Hyer and B. Sander, *Simulating quantum dynamics on a quantum computer* Journal of Physics A: Mathematical and Theoretical, vol. 44, num. 44, 2011

[10] C. Laumann, R. Moessner, A. Scardicchio, and S. Sondhi, *Quantum annealing: The fastest route to quantum computation?*, European Physics Journal Special Topics, 224, 75, 2015

[11] H. Wang, S. Ashhab and F. Nori, *Quantum algorithm for simulating the dynamics of an open quantum system*, Phys. Rev. A 83, 062317, 2011

[12] M. Scully, M. Zubairy, *Quantum Optics* Cambridge University Press: Cambridge, 1997

[13] B. Terhal and D. DiVincenzo, *Problem of equilibration and the computation of correlation functions on a quantum computer*, Phys. Rev. A 61, 022301, 2000

[14] H. Wang, *Quantum algorithm for obtaining the eigenstates of a physical system*, Phys. Rev. A 93, 052334, 2016

[15] J. Biamonte and P. Love, *Realizable hamiltonians for universal adiabatic quantum computers*, Physical Review A 78, 012352, 2008

[16] J. Biamonte, *Non-perturbative k-body to two-body commuting conversion hamiltonians and embedding problem instances into Ising spins*, Physical Review A 77, 052331, 2008

[17] W.Z. Liu, J.F. Zhang, Z.W. Deng, and G.L. Long, *Simulation of general three-body interactions in a nulcear magnetic resonance ensemble quantum computer*, Science in China Series G: Physics, Mechanics and Astronomy,vol. 51, pages 1089-1096, 2008

[18] M. Cetina, A. Bylinskii, L. Karpa, D. Gangloff, K.M. Beck, Y. Ge, M. Scholz, A.T. Grier, I. Chuang and V. Vuletic, *One-dimensional array of ion chains coupled to an optical cavity*, New Journal of Physics, vol. 15, pages 053001, 2013

[19] A. Messiah,*Quantum Mechanics*, Vol. II, Amsterdam: North Holland; New York: Wiley (1976).

[20] T. Wong and D. Meyer, *Irreconcilable Difference Between Quantum Walks and Adiabatic Quantum Computing*, Physical Review A, 93, 062313, 2016

[21] M. Mézard, G. Parisi, and R. Zecchian, *Analytic and algorithmic solution of random satisfiability problems*, vol. 297, issue 5582, pages 812-815, 2002

[22] J. Crawford and L. Auton, *Experimental results on the crossover point in satisfiability problems*, proceedings of the 11th National Conference on AI , pages 21-27, 1993

[23] D. Mitchell, B. Selman, and H. Levesque. *Hard and easy distributionsof SAT problems*, proceedings of the 10th National Conference on AI, pages 459-465, 1992

[24] B.A. Huberman and T. Hogg. *Phase transitions in Artificial Intelligence systems*, Artificial Intelligence , 33, pages 155-171, 1987

[25] B. Garraway, *The Dicke model in quanutm optics: Dicke model revisited*, Phil. Trans. R. Soc. A 369, pages 1137-1155, 2011

[26] S. Ghoreishi, M. Sarbishaei and K. Jvidan, *Entanglement between two Tavis-Cummings systems with $N = 2$*, International Journal of Theoretical and Mathematical Physics, 2(6), pages 187-195, 2012

[27] L. Horvath and B. Sanders, *Photon coincidence spectroscopy for two-atom cavity quantum electrodynamics*, Journal of Modern Optics, vol. 49, issue 1-2, 2002